The evolutionary dynamics and conservation of the secondary structure of ITS rDNA vary across the different haplotypes of *Lentinula edodes* that are globally distributed.

Mohammed M. Hawash*, Nadher A. Abed, Y. A. Obaid

Directorate of Anbar Educational, Ministry of Education ,Anbar, Iraq
***** (Email: mohammed.hawwash2102@sc.uobaghdad.edu.iq)

Abstract
This study relied on an integrated analysis of sequence characteristics, haplotype diversity, phylogenetic relationships, RNA secondary-structure modelling, and paired-site screening to analyse ITS rDNA variation and structural conservation across 19 geographically diverse Lentinula edodes accessions, including three from Iraq. A crucial component of fungal ITS evolution is the evolutionary accommodation of nucleotide diversity within structurally constrained ribosomal RNA sections. The ITS sequences were aligned, yielding 567 locations, with 330 remaining after gaps and incomplete data were eliminated. Seven haplotypes were discovered, with a haplotype diversity of 0.544 ± 0.136 and a nucleotide diversity of 0.03931 ± 0.03120. This reveals significant sequence variation among the analysed accessions. Given this distinction, both RNAfold and RNAalifold projected a well-conserved stem-loop structure. The consensus structure is anticipated to be thermodynamically stable (MFE = −263.78 kcal/mol; ensemble free energy = −272.45 kcal/mol), with a high level of concordance established across haplotypes (Pearson r = 0.995, P < 0.001). The expected stability of haplotype-specific structures differed; the Iraqi Maysan accession demonstrated somewhat less stability, whereas the Nepalese accession had the maximum stability. After screening 6,903 variable-site pairings, lineage-specific GC–CG state reversals were discovered; however, these were restricted to a single haplotype and did not exhibit statistical evidence for compensatory covariation. Overall, outcomes reveal that ITS sequence variation in *L. edodes* is accommodated within a projected RNA structural framework that is largely retained in the absence of direct evidence of compensatory evolution.

Keywords. Haplotype, ITS rDNA, *L. edodes*, Molecular evolution, Phylogenetics, RNA folding, Secondary structure.

1. Introduction

Mushroom-forming fungi are a varied group of organisms that serve vital ecological, nutritional, and commercial functions. Shiitake mushrooms or *Lentinula edodes* (Berk.) Pegler is one of the most commonly farmed and consumed edible mushrooms in the world. This East Asian natural fungus, which contains polysaccharides, dietary fibres, antioxidants, and other bioactive compounds, has long been grown and is known for its nutritional and functional properties [1; 2]. Aside from its commercial importance, *L. edodes* is a varied lineage with a complicated global diversification history. Significant evolutionary variety within *Lentinula* has been identified by recent phylogenomic and population genomic analyses, with spatially structured lineages influenced by domestication processes, historical biogeography, and environmental adaptability [3; 4]. These revelations point out the importance of molecular approaches in comprehending genetic diversity and evolutionary relationships among geographically diverse groups.

The nuclear ribosomal DNA internal transcribed spacer (ITS) region is a frequently used molecular marker in fungal systematics and evolutionary research. The ITS region, which includes ITS1, the 5.8S rRNA gene, and ITS2, combines conserved structural features with variable areas that offer crucial information for phylogenetic reconstruction, species identification, and genetic diversity assessment [5; 6; 7; 8]. ITS is now the universal DNA barcode for fungus and is frequently employed in research on fungal evolution and population differentiation.

The internal transcribed spacer (ITS) region of mushroom-forming fungi has been proven to be useful for evaluating genetic diversity, phylogenetic relationships, species identification, and evolutionary patterns in earlier research. Phylogenetic and population-genomic analyses of the genus *Lentinula* have identified spatially structured lineages and significant evolutionary diversity in *L. edodes* and related species [3; 4; 24]. Previous research on the 5.8S rRNA region of *L. edodes* also showed that ribosomal sequence characteristics were conserved [13]. In addition to offering a fungal-specific framework for evaluating ITS sequence and structural diversity, these studies collectively demonstrate the value of ITS and associated ribosomal markers for analysing genetic variation and evolutionary relationships in *Lentinula*.

The structural impacts of sequence divergence have not gotten as much attention as nucleotide variation, despite the fact that ITS analyses have proven useful in finding patterns of fungal diversity and phylogenetic relationships. The need to preserve particular secondary structures may limit the evolutionary modifications of ribosomal DNA segments that contribute to functional RNA molecules. Therefore, studying RNA folding patterns in addition to sequence change can help us better understand the mechanisms that maintain functioning ribosomal architecture throughout evolution. Previous research has documented the conservation of ribosomal structural characteristics in *L. edodes*. As a result, researching RNA folding patterns as well as sequence change can help us better understand the mechanisms that keep the ribosomal architecture functional during evolution. Previous research has revealed that the structural properties of ribosomes are retained in *L. edodes.*

Prior studies established that the relationship between ITS sequence variation and secondary structure conservation across worldwide haplotypes is still unclear despite much research on the phylogeny and genetic diversity of *L. edodes*. Thus, the current study integrated sequence variation analysis, haplotype characterisation, phylogenetic reconstruction, and RNA secondary structure prediction to evaluate the structural and evolutionary features of ITS rDNA among geographically distinct *L. edodes* haplotypes. The structural features of ribosomes are maintained in *L. edodes*. This method offers fresh perspectives on how structural conservation and nucleotide variability are balanced throughout fungal ribosomal DNA evolution.

2. Materials and methods

2.1. Sequence dataset and alignment

A set of 19 ITS rDNA sequences of *Lentinula edodes* from various geographic locations were retrieved from the NCBI GenBank database. The database contained reference sequences from various regions of the world as well as three Iraqi accessions (Table 1). MEGA version 12 [15] employed the MUSCLE method [14] for aligning multiple sequences. The resulting alignment was manually reviewed and modified as necessary to guarantee positional homology before additional investigation.

2.2. RNA secondary structure prediction and consensus structure analysis

To evaluate structural variation and conservation within the ITS region, RNA secondary structures were predicted for representative sequences of the identified haplotypes using the ViennaRNA Package's RNAfold function [16]. Predictions were made at 37°C with the default settings. Each haplotype was assigned a minimum free energy (MFE), ensemble free energy, and ensemble diversity value. Moreover, RNAalifold [17] was employed to create a consensus secondary structure from the entire ITS alignment by integrating

sequence conservation and covariation signals across aligned sequences. To measure the degree of structure conservation across haplotypes, consensus structural metrics such as MFE and covariance contribution were used.

Table 1: Lists the nuclear ribosomal DNA sequences' origin, accession number (ID), and length from *Lentinula edodes* populations worldwide.

No.	Country	Code	GenBank accession	Sequence length (bp)
1	Austria	AUT	PX956995	732
2	Belgium	BEL	PV107748	704
3	China	CHN	MH997454	675
4	India	IND	PX457878	642
5	Iran	IRN	PP498976	667
6	Iraq (Baghdad)	IRQ-BAG	OM432157	676
7	Iraq (Mosul)	IRQ-MOS	OR346010	658
8	Iraq (Maysan)	IRQ-MAY	MW375037	434
9	Japan	JPN	PV107999	698
10	Laos	LAO	MT252553	655
11	Mexico	MEX	PV083830	691
12	Nepal	NPL	PZ395648	747
13	Nigeria	NGA	OM252524	603
14	Poland	POL	EF174453	724
15	Russia	RUS	OP508316	749
16	South Korea	KOR	PZ545925	693
17	Taiwan	TWN	MH444818	730
18	Thailand	THA	PZ395649	746
19	USA	USA	OQ539569	580

2.3. Phylogenetic analysis

The phylogenetic relationships between *L. edodes* accessions were reconstructed using the Maximum Parsimony (MP) method in MEGA version 12 [15]. After the aligned ITS sequences were utilised to generate the most parsimonious tree, branch support was evaluated using bootstrap analysis with 1000 repetitions. The resulting topology was applied to investigate haplotype relationships as well as the association between sequencing divergence and structural variation.

2.4. Haplotype identification and network construction

DnaSP version 5 was used to assess haplotype diversity in the ITS dataset [18]. To identify unique haplotypes, nucleotide variation patterns were employed, and the relationships between haplotypes were reconstructed using NETWORK software's Integer Neighbor-Joining technique (19). PopART [20] was used to display the resulting haplotype network, revealing genetic linkages and mutational differences between global haplotypes.

2.5. Neutrality statistics test and genetic diversity

Tajima's D, Fu and Li's D*, Fu and Li's F*, Fu's Fs, and Strobeck's S were employed to evaluate deviations from neutral expectations. Neutrality statistics were viewed as descriptive evidence of non-neutral or non-equilibrium patterns in the sampled dataset rather than as conclusive tests of demographic history because the sample only included 19 accessions with uneven geographic representation. Statistics for genetic diversity included the number of segregating sites, total mutations, GC content, haplotype number, haplotype diversity (Hd), nucleotide diversity (Pi), and average pairwise nucleotide differences (k).

2.6. A quantitative comparison of thermodynamic attributes

obtained a value for the three thermodynamic variables among the seven typical haplotypes. Pearson correlations were computed using the seven haplotype values, with two-tailed P values provided. Spearman rank correlations were also conducted as a sensitivity analysis due to the small effective sample size (n = 7). These associations were viewed as exploratory rather than population-level statistical relationships. Because accession lengths ranged, correlation data were interpreted as relationships between sequence-dependent folding predictions rather than direct assessments of intrinsic RNA stability.

2.7. Exhaustive paired-site covariance assessment

The aligned FASTA contained 19 sequences and 567 alignment positions. All alignment columns were checked; columns with gaps or unclear nucleotides were removed from the initial paired-site screen, leaving 330 gap-free places, 118 of which were variable. All 6,903 pairwise combinations of these variable locations were investigated. Each pair's nucleotide-state combinations, number of distinct pair states, canonical base-pair states, and mutual information were obtained. The proposed compensatory-like patterns were defined as changes between canonical paired states (GC↔CG), rather than statistically validated compensatory replacements. To reduce pseudoreplication, similar patterns appeared at the seven-haplotype level.

3. Results and Discussions

3.1. Secondary structure analysis of ITS rDNA haplotypes

3.1.1. Consensus secondary structure of global ITS sequences

Despite nucleotide variation among geographically different accessions, matching 19 global ITS rDNA sequences of *L. edodes* yielded a well-preserved folding pattern (Figure 1). Table 2 shows that the consensus structure has an ensemble free energy of -272.45 kcal/mol and a minimum free energy (MFE) of -263.78 kcal/mol, indicating a thermodynamically stable RNA folding pattern within the analysed ITS dataset. The lower ensemble free energy in comparison to the consensus MFE implies the presence of alternative energetically favourable conformations within the thermodynamic ensemble, displaying structural flexibility while maintaining overall folding stability. The consensus structure had a significant covariance contribution (−151.76 kcal/mol), suggesting that paired portions of the RNA structure may be conserved due to nucleotide alterations across matched sequences. Covariation, or the capacity of interacting nucleotides to undergo coordinated substitutions while retaining base-pairing links, is an important aspect of the formation of RNA structure. The significant covariance signal observed in the current

analysis indicates that structural constraints that maintained conserved folding patterns across worldwide *L. edodes* accessions may have had an impact on evolutionary changes within the ITS region rather than being wholly random. ITS evolution in *L. edodes* may be controlled by a balance between nucleotide diversity and structural stability, according to the maintenance of a comparable secondary structure despite sequence divergence. Although structural limitations may prevent disruptive mutations that alter the structure of RNA folding, sequence polymorphisms help with phylogenetic resolution and haplotype distinction. Therefore, by identifying conserved structural features that have persisted during species diversification, secondary structure analysis offers extra evolutionary information beyond conventional sequence-based methods.

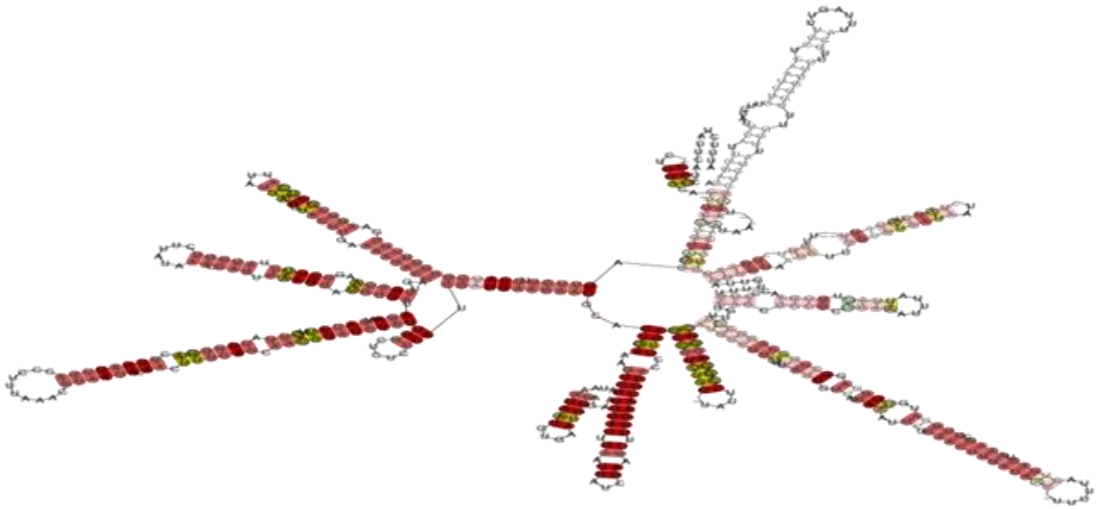


Figure 1: By aligning 19 *L. edodes* sequences with RNAalifold, the consensus secondary structure of the ITS rDNA region was predicted. Despite sequence diversity, the structure displays conserved stem-loop motifs. A conserved base-pair type with no sequence variation is represented by red in the RNAalifold colour scheme, several compatible base-pair types are shown by yellow/ochre, and lower structural conservation is indicated by faint colours when some sequences are unable to form the consensus base pair.

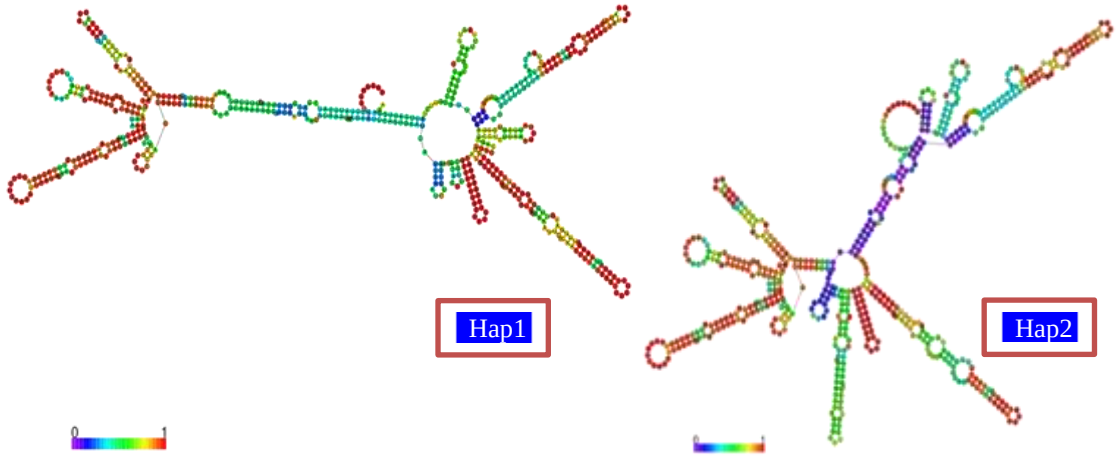
Table 2: Presents the thermodynamic details of the consensus ITS rDNA secondary structure derived from the alignment of 19 *L. edodes* sequences.

Parameter	Value
Number of sequences	19
Alignment length	567 bp
Consensus MFE	−263.78 kcal/mol
Covariance contribution	−151.76 kcal/mol
Ensemble free energy	−272.45 kcal/mol

3.1.2. Secondary structure diversity and conservation among ITS haplotypes

In fact, although the consensus structure revealed significant structural conservation across the whole dataset, the thermodynamic properties of individual haplotypes differed (Figure 2; Table 3). From −97.60 kcal/mol in the Iraqi Maysan accession to −154.60 kcal/mol in the Nepalese accession, the projected MFE values varied among geographically different haplotypes. Greater advantageous predicted folding energies are indicated by greater negative MFE values; however, sequence length also has a significant impact on these values. The larger MFE of Hap3 should not be taken as proof of intrinsically worse RNA stability because the Iraqi Maysan sequence is significantly shorter (434 bp) than the Nepalese version (747 bp). Instead, comparisons between haplotypes should be evaluated cautiously because the MFE difference reflects, at least partially, the significant variation in sequence length.

Estimates of ensemble free energy showed a similar pattern, with values between -106.50 and -165.85 kcal/mol. While the significantly greater value seen for Iraqi Maysan admission suggests a less favourable folding ensemble, the lowest ensemble free energy achieved for Nepalese accession contributes to the resulting higher degree of thermodynamic stability. These results suggest that local folding energetics are impacted by nucleotide differences across *L. edodes* haplotypes without appreciably changing the overall ITS structural framework. Ensemble diversity values ranged from 78.08 in the Iraqi Maysan accession to 123.70 in the Iraqi Baghdad accession. Lower values indicate a more confined folding landscape, whereas higher ensemble diversity reveals a wider range of possible alternative conformations, implying greater structural flexibility. The increased diversity observed in the Iraqi (Baghdad) and Thai accessions suggests greater conformational flexibility than haplotypes with lower diversity values. The general stem-loop architecture of every haplotype under investigation stayed mostly unchanged in spite of these thermodynamic alterations. Instead of drastically rearranging the overall architecture, structural variation was typically restricted to localised features like loop size, stem length, and branching patterns. This finding implies that ITS evolution in L. edodes requires finding a compromise between structural conservation and sequence variety. Despite sequence diversity, it has been demonstrated that ribosomal DNA secondary structures in *L. edodes* are maintained. The significance of structural restrictions on ribosomal RNA organization was highlighted by Kwan et al. [14], who observed notable similarities between the predicted secondary structure of the 5.8S rRNA region in *L. edodes* and those of other fungi and distant eukaryotic species. Barroso *et al*. [21] claim that ribosomal RNA structures in Agaricales have mostly not changed over the course of evolution, with most sequence changes taking place within certain regions while maintaining the fundamental structural foundation. The ITS sections of many ectomycorrhizal basidiomycetes contain structurally conserved RNA components, such as embedded signal recognition particle (SRP) RNA sequences, according to Rosenblad *et al.* [22]. However, no such structural insertion was found in the current *L. edodes* dataset. The uniform folding pattern observed across haplotypes, on the other hand, lends credence to the notion that ITS evolution is dictated by RNA structural constraints. ITS evolution in *L. edodes* is often marked by significant sequence diversity while retaining the core structural framework, as determined by haplotype variation, thermodynamic parameters, and projected RNA secondary structures. The findings show how important secondary structure analysis is for improving phylogenetic and haplotype-based approaches and furthering our understanding of the molecular evolution of fungal ribosomal DNA.



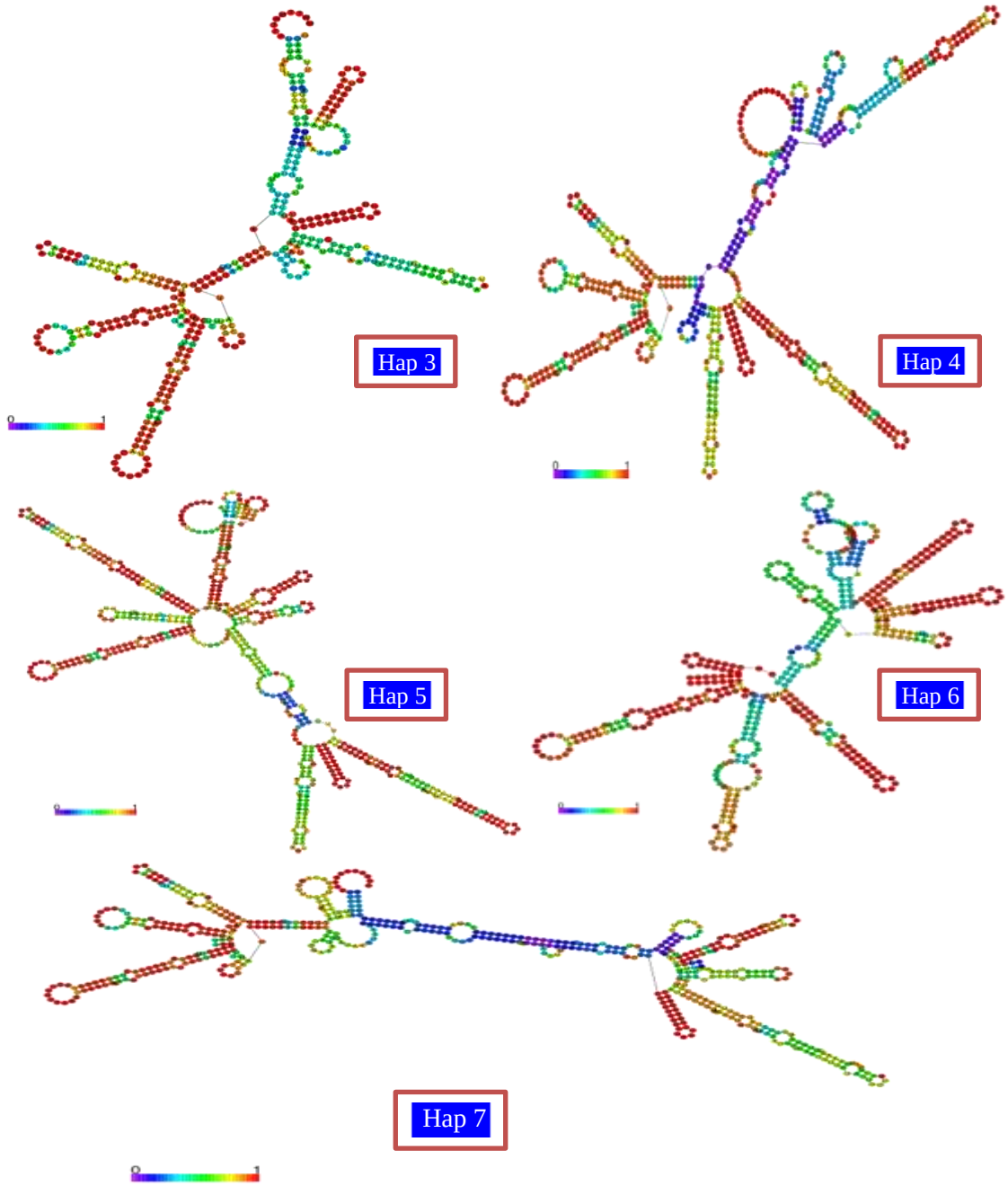


Figure 2. The anticipated MFE secondary structures of the seven ITS haplotypes found in *L. edodes*. The colour scale of 0 to 1 depicts base-pairing probabilities, with higher values suggesting a higher anticipated pairing probability.

Table 3: Thermodynamic characteristics of *L. edodes* secondary structures predicted by the ITS haplotype.

Haplotype	Representative accession	MFE (kcal/mol)	Ensemble free energy (kcal/mol)	Ensemble diversity
Hap 1	Iraqi Mosul	−145.70	−157.50	112.33
Hap 2	Iraqi Baghdad	−140.90	−152.94	123.70
Hap 3	Iraqi Maysan	−97.60	−106.50	78.08
Hap 4	Japanese	−144.90	−156.89	106.47
Hap 5	Nepalese	−154.60	−165.85	91.36
Hap 6	Nigerian	−138.20	−144.68	83.17
Hap 7	Thai	−138.30	−150.26	122.85

3.2. Phylogenetic relationships and their association with ITS secondary structure variation

The *L. edodes* accessions from various locations had close evolutionary ties, according to the phylogenetic analysis based on the ITS rDNA sequence. All accessions were assigned to a single main lineage, confirming their categorisation as members of the same species. However, a large number of internal clusters revealed that geographically different accessions differed genetically (Figure 3). The ITS region of *L. edodes* is well conserved across geographically diverse populations, as evidenced by the discovery of Iraqi accessions, including Baghdad and Maysan clones, in the major phylogenetic cluster among other worldwide accessions. Nigerian and Nepalese accessions, on the other hand, were discovered in more distinct locations, suggesting greater sequence diversity in the dataset. ITS secondary structural features were used to assess the detected phylogenetic divergence. All predicted topologies had a similar overall stem-loop organization (Figure 2), despite haplotype differences in thermodynamic metrics like minimum free energy (MFE), ensemble free energy, and ensemble diversity (Table 3). This demonstrates that the overall ITS folding architecture was not significantly impacted by nucleotide changes introduced during evolutionary diversification.

The Iraqi Maysan lineage had a higher MFE value (−97.60 kcal/mol), whereas the Nepalese lineage had the lowest (−154.60 kcal/mol). Although the Maysan sequence is substantially shorter (434 bp) than the Nepalese sequence (747 bp), the MFE difference should be considered in relation to sequence length rather than as a direct indicator of inherent folding stability. Nonetheless, both haplotypes maintained the conserved structural pattern observed in every sequence analysed, indicating that sequence variations occurred within a largely intact RNA folding framework.

This analysis demonstrated a relationship between sequence divergence and structural conservation, which is consistent with previous research revealing the evolutionary relevance of the ITS secondary structure. Coleman [23] reports significant nucleotide diversity throughout ITS2 evolution in eukaryotes while keeping unique RNA structural features. According to this hypothesis, evolutionary changes are often concentrated in variable regions, whereas conserved structural features endure because of functional constraints related to ribosomal RNA processing. In Agaricales, ribosomal RNA evolves by localised sequence changes that preserve the molecular structural core, as described by Barroso *et al*. [21]. Rosenblad *et al*. [22] identified conserved RNA segments in the ITS sequences of various basidiomycete species, highlighting the structural complexity of fungal ITS sections. The continuous stem-loop structure among haplotypes lends credence to the notion that RNA structural restrictions influence ITS evolution, despite the fact that no such structural insertion was discovered in the current *L. edodes* dataset.

Phylogenetic clustering and secondary structure conservation are consistent, implying that genetic diversity and structural organization preservation are maintained throughout *L. edodes*' ITS evolution. Conserved RNA folding patterns disclose more about the evolutionary stability of ribosomal DNA sections, although nucleotide variation provides phylogenetic information for distinguishing evolutionary lineages.

Recent genomic data indicates the existence of evolutionary differentiation in *L. edodes*. Sierra-Patev *et al*. [24] reported that *L. edodes* comprises several genetically differentiated evolutionary lineages spread over Asia, including a separate Nepalese

lineage that is a divergent branch from other populations. The distinct location of the Nepalese haplotype identified in the current ITS study is thus compatible with larger genomic data demonstrating long-term evolutionary divergence within the species. Overall, the combination of phylogenetic and RNA secondary structure analysis revealed that significant structural conservation and sequence diversification are traits associated with ITS evolution in *L. edodes*. Despite a rise in genetic variety among geographically diverse lineages, this pattern emphasises the necessity of structural constraints in preserving RNA folding stability.

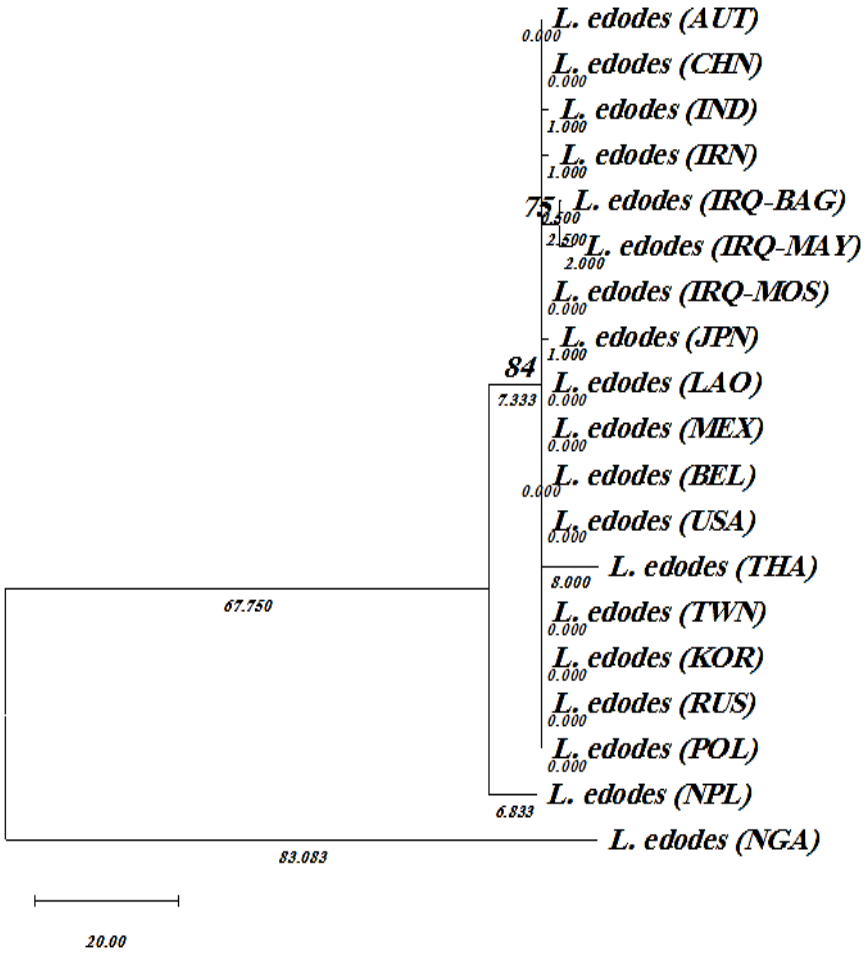


Figure 3: Maximum Parsimony phylogeny demonstrating the genetic relationships between regionally diverse ITS haplotypes of *L. edodes*.

3.3. Haplotype relationships and their association with phylogenetic and secondary structure analyses

Among the *L. edodes* accessions under investigation, the haplotype network analysis identified seven ITS rDNA haplotypes (Figure 4). The network showed a star-like structure with a central haplotype holding the core location and connecting to the other haplotypes by a restricted number of mutational steps. This pattern implies that diversification has taken place through the accumulation of a small number of nucleotide changes and that the examined haplotypes have a very recent shared genetic background. The center position of this haplotype shows that it belongs to a common or ancestral-like lineage in the dataset being analysed. The arrangement of peripheral haplotypes around the dominant core haplotype indicates that geographically

scattered accessions reveal significant genetic differentiation while maintaining overall genetic cohesiveness. Although most haplotypes were separated from the center lineage by only a few mutational steps, the Nigerian accession was the most divergent in the haplotype network, with the most mutational changes. This pattern was aligned with the phylogenetic analysis, which indicated the Nigerian accession (Hap6) to represent one of the most divergent lineages within the species. However, all accessions remained assigned to a single species-level clade, thus implying that the observed divergence is attributable to intraspecific evolutionary differences rather than species isolation.

The relationship between haplotype differentiation and ITS secondary structural diversity suggests that sequence diversity occurred without severely affecting RNA folding organization. All predicted a secondary structure with a surprisingly similar stem-loop form, despite the fact that nucleotide alterations resulted in seven unique haplotypes (Figure 1). Instead of considerable variations in the overall folding pattern, structural differences between haplotypes were mostly represented by thermodynamic metrics such as minimum free energy (MFE), ensemble free energy, and ensemble diversity (Table 3). The Iraqi Maysan accession (Hap3) had a higher MFE value (−97.60 kcal/mol), indicating decreased folding stability. The Nepalese accession (Hap5) had the lowest MFE value (−154.60 kcal/mol), indicating the most thermodynamically favourable predicted structure among the haplotypes studied. Nonetheless, both haplotypes preserved the essential structural basis observed across the dataset. Although the conserved structure is consistent with structurally accommodated nucleotide change, the paired-site study did not offer enough independent evidence to confirm compensatory substitutions as the mechanism that maintains this structural order.

Indeed, ITS evolution in *L. edodes* is characterised by a balance between sequence diversity and structural constraint, according to the haplotype network, phylogenetic clustering, and secondary structure conservation. While nucleotide variation resulted in many haplotypes and obvious phylogenetic divergence, the conserved secondary structure implies that evolutionary changes are controlled by ribosomal DNA organization and RNA processing requirements. The existence of seven ITS haplotypes in the current global dataset suggests significant genetic variety, particularly when contrasted to research on geographically confined populations. This variety matches up with previous genome studies that revealed multiple evolutionary lineages related to long-term divergence and regional variation in L. edodes. Within *L. edodes* sensu lato, Sierra-Patev *et al*. [24] discovered spatially organised lineages of evolution, including a unique Nepalese lineage that was phylogenetically distant from the other populations. Three genetically separate subgroups of *L. edodes* were determined by Zhang *et al*. [4] employing genome-wide population genomic data. The hypothesis that the ITS variation observed in the current study implies more extensive evolutionary processes influencing genetic differentiation within the species is supported by these genomic data. A thorough understanding of molecular evolution *in L. edodes* is generally revealed by combining haplotype connections, phylogenetic reconstruction, and RNA secondary structure studies. This pattern highlights the significance of integrating sequence-based and structure-based methods for comprehending the evolutionary history of fungi by establishing that ITS diversification happens through the accumulation of nucleotide variation while maintaining conserved structural features.

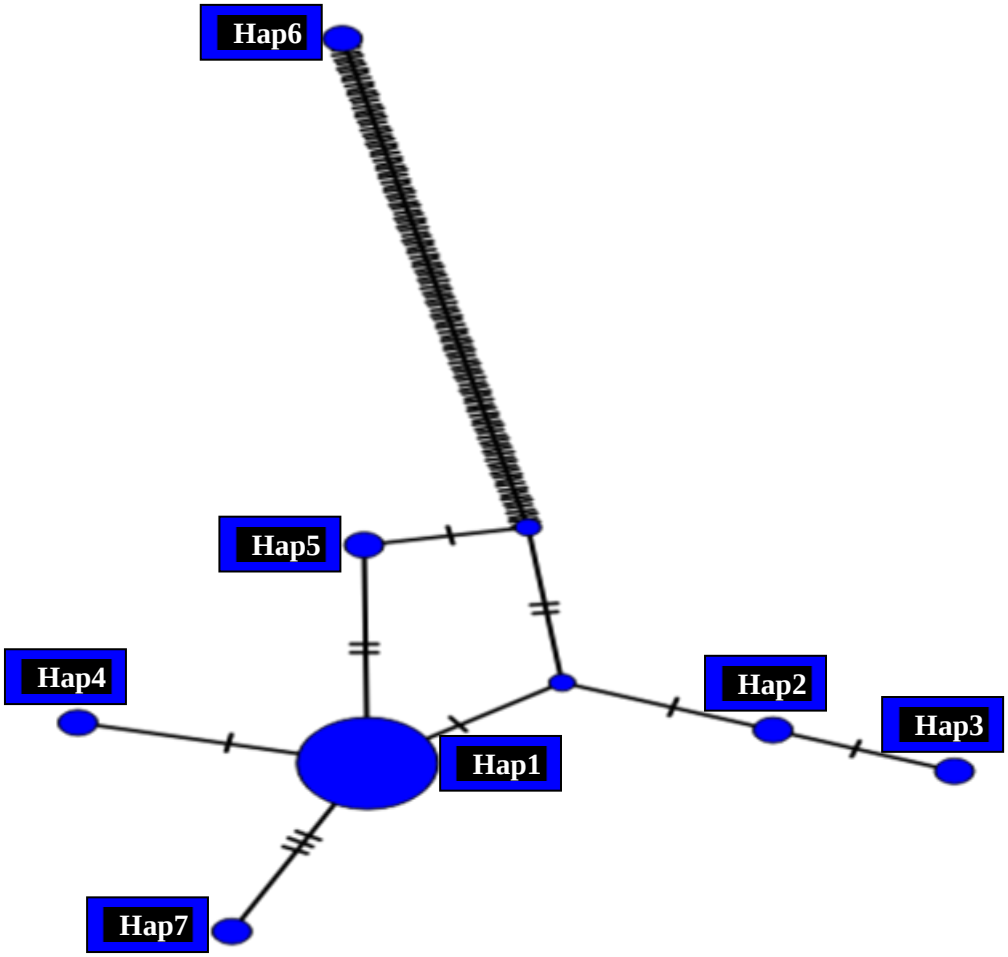


Figure 4. The global *Lentinula edodes* haplotype network is based on ITS. The size of the blue circles represents haplotype frequency, whilst hatch marks along connecting branches represent the number of mutational steps between haplotypes. Small unlabelled blue circles represent estimated median vectors reflecting unsampled or potential ancestral haplotypes added during network reconstruction. Hap1 corresponded to the Austrian, Belgian, Chinese, Indian, Iranian, Iraqi (Mosul), Laotian, Mexican, Polish, Russian, South Korean, Taiwanese, and American accessions; Hap2 to the Iraqi (Baghdad) accession; Hap3 to the Iraqi (Maysan) accession; Hap4 to the Japanese accession; Hap5 to the Nepalese accession; Hap6 to the Nigerian accession; Hap7 to the Thai accession.

3.4. Relationship between haplotype divergence, phylogeny, and RNA secondary structure

The observed variation in ITS secondary structures was broadly consistent with the genetic differentiation exhibited by both the phylogenetic tree and haplotype investigations. Although the seven detected haplotypes differed in thermodynamic parameters such as MFE, ensemble free energy, and structural diversity, they all had a substantially preserved stem-loop structure. This finding suggests that ITS structural evolution in *L. edodes* occurred concurrently with nucleotide sequence divergence while maintaining the fundamental RNA folding framework.

In fact, the recognised nucleotide polymorphisms in the ITS region may contribute to localised alterations in secondary-structure elements, particularly in stem-loop areas, while the overall structural framework remains rather stable. Rampersad's [25] observation that fungal

ITS sections may exhibit sequence and secondary-structure modification while maintaining conserved structural features is in agreement with this result. Lal et al. [26] highlighted the structural consequences of nucleotide variation by reporting that nucleotide changes inside stem-loop regions can modify local structural features and impair conformational stability. Their study supports the hypothesis that sequence variation can affect local nucleic acid structure and stability even though it mainly focused on nanovirus stem-loop structures instead of fungal ITS regions.

However, sequence divergence within ribosomal DNA areas is often accompanied by changes in RNA secondary structure, demonstrating evolutionary variety among fungal species, according to González and Labarère [27]. Likewise, Gillespie [28] emphasised the differences in evolutionary behaviour between stem and loop sections, such as hairpin expansion and contraction, which can contribute to sequence-length variation. Consistent with these results, the current analyses revealed that *L. edodes* haplotypes with divergent sequences and thermodynamic properties retained significant structural similarity, implying that sequence diversification may occur alongside conservation of the overall secondary-structure framework. The highly stable consensus structure obtained from RNAalifold and the notable conservation of the overall ITS folding pattern suggest that structural constraints played a critical role in the genesis of *L. edodes*. Therefore, rather than being random variations in RNA folding, the structural differences between haplotypes are more likely to be evolutionary changes gathered via lineage branching.

3.5. Genetic diversity and neutrality tests

The ITS alignment had 567 sites, with 330 left after gaps and insufficient data were removed. There were 118 variable sites and 119 mutations identified. The overall G+C content was 39.7%, as indicated in Table 4. Seven haplotypes were observed, with 0.544 ± 0.136 haplotype diversity, 0.03931 ± 0.03120 nucleotide diversity, and an average nucleotide difference of 12.97076. The results suggest that the sampled accessions had high sequence variation. Neutrality tests revealed that Tajima's D = -2.579 ($P < 0.001$), Fu and Li's D* = -3.899, and Fu and Li's F* = -4.083 ($P < 0.02$). The negative values indicate that there are more unusual types than the corresponding neutral equilibrium models' assumptions permit. This pattern can be caused by demographic expansion, purifying selection, population partition, or other deviations from model assumptions; statistics cannot distinguish between various scenarios. Fu's Fs was positive (5.949), Strobeck's was 0.011, and the observed haplotype distribution was predicted with $P = 0.009$. The highly low Tajima's D and Fu and Li statistics contrast with the positive Fu's Fs, suggesting that the neutrality tests shouldn't be taken as independent proof of recent population growth. Rather, in a geographically diverse sample, the data demonstrate a departure from the neutral assumptions of the tests (Table 4).

Table 4. Genetic diversity and neutrality tests for the 19 *L. edodes* ITS accessions.

Parameter	value
Alignment length	567 bp
Sites excluding gaps/missing data	330 bp
Variable sites (S)	118
Total mutations (Eta)	119
G+C content	39.7%
Number of haplotypes (h)	7
Haplotype diversity (Hd)	0.544 ± 0.136
Nucleotide diversity (Pi)	0.03931 ± 0.03120
Mean nucleotide differences (k)	12.97076
Tajima's D	−2.57871*
Fu & Li's D*	−3.89942
Fu & Li's F*	−4.08314
Fu's Fs	5.949
Strobeck's S	0.011

3.6. Exhaustive paired-site covariance analysis

The entire 567-position alignment was screened for paired sites. After removing columns with gaps or confusing characters, 330 homologous positions remained, including 118 variable sites. These produced 6,903 pairwise pairings. Among the 19 accessions, sixteen site pairs revealed at least two canonical RNA base-pair states. However, the majority of these signals matched the same lineage-specific GC↔CG pattern linked with the Nigerian accession; therefore, they cannot be considered independent compensating events. The most noticeable pattern occurred at locations 32-212, where GC appeared in 18 accessions and CG in the Nigerian accession; the same lineage-specific state reversal was noted in other related site combinations (Table 5).

At the seven-haplotype level, the canonical GC-CG reversals were limited to a single haplotype rather than being duplicated over several haplotypes. Two other site combinations (380-387 and 47-384) exhibited simultaneous mutations at two sites in more than one haplotype, but their alternative states were noncanonical (e.g., GG, AA, and TA) and so do not support compensatory base-pair evolution.

Table 5. Summarises the comprehensive paired-site covariance screening of the 567-position ITS alignment.

Screening metric	Value
Variable-site pair combinations	6,903
Pairs with ≥2 canonical pair states	16
Conservative evidence for independent compensatory evolution	None

In fact, the mutual data was effective in rating nucleotide relationships, but the highest values were frequently caused by infrequent lineage-specific alterations rather than recurring paired-state changes. As a result, the current analysis does not support the assertion of statistically verified compensating substitutions. Instead, the observed GC↔CG reversals are best defined as potential compensatory-like patterns that are consistent with, but do not independently establish, structural conservation.

3.7. Integrated analysis of sequence divergence and RNA structure

The sequencing, haplotype, phylogenetic, secondary-structure, and paired-site screening experiments reveal that the sequences of *L. edodes* accessions have significant nucleotide variability while keeping a broadly comparable projected ITS structural framework. The fundamental contribution of this study is a thorough examination of sequence diversification in relation to projected structural conservation, as well as an explicit distinction between descriptive paired-site interactions and statistically supported covariation. This distinction is especially important since frequent linkages between sequence states might result from lineage-specific substitutions and should not always be interpreted as evidence of separate compensating substitutions.

The present results support structural conservation as a comparative observation rather than a proven mechanistic limitation. The regularity of stem-loop organization across the seven analysed haplotypes supports structural constraint, but prediction cannot indicate biological function or selective maintenance.The thorough paired-site analysis noticed many lineage-specific GC↔CG reversals, but they were primarily confined to one haplotype, providing insufficient independent evidence for statistically supported compensating covariation. Thus, covariation analysis improves the description of structurally compatible sequence change while avoiding compensatory evolution. The results are broadly consistent with previous studies that found structural conservation in fungal

ribosomal RNA [21, 22, 25, 27, 28], as well as genetic evidence for spatially structured evolutionary differentiation in *L. edodes* [3, 4, 24]. The Nepalese accession's unique position in the current dataset is therefore interesting, but it should be seen as a pattern in the sampled ITS data rather than independent proof for a discrete evolutionary lineage.

Conclusion

This study proves that nucleotide changes accumulate in the ITS rDNA region of *L. edodes*, whereas the haplotypes studied retain a widely conserved RNA secondary-structure architecture. Despite differences in sequence and thermodynamics, all seven haplotypes had a similar stem-loop structure. The comprehensive paired-site analysis revealed lineage-specific GC–CG reversals without enough independent or statistical evidence to establish compensatory substitutions as a proven mechanism, but the predicted structures and the strong covariance contribution of the consensus structure are consistent with structural conservation. Therefore, while avoiding the stronger assertion that compensatory substitutions were essential in maintaining RNA-folding stability, the current findings support structural conservation as a significant comparative aspect of ITS evolution. Sequence variation, phylogenetic relationships, haplotype differentiation, and secondary-structure conservation all agree, which emphasises the importance of combining sequence-based and structure-based investigations to gain a deeper understanding of the evolutionary dynamics of fungal ITS regions.

This study reveals that under severe structural constraints, nucleotide substitutions accumulate in the ITS rDNA region of *L. edodes* without significantly altering the thermodynamic stability and conserved architecture of the RNA secondary structure. All seven distinct haplotypes retained a conserved stem-loop topology despite clear genetic and thermodynamic variation, confirming that sequence evolution preserves functionally significant structural characteristics. Throughout the evolutionary history of the species, compensatory substitutions were crucial in preserving the stability of RNA folding, as evidenced by the strong association found in the consensus structure. The substantial association between phylogenetic relationships, haplotype structure, and RNA secondary structure conservation highlights the evolutionary importance of structural constraints in influencing ribosomal DNA evolution. Overall, the results provide novel perspectives on the interaction between structural conservation and sequence diversification within fungal ITS regions, emphasising the importance of combining secondary-structure analyses with traditional molecular evolutionary techniques to gain an improved grasp of fungal evolutionary dynamics.

Acknowledgements

The authors express appreciation to the researchers who donated ITS sequences to GenBank. These publicly available data were critical to our analysis, demonstrating the value of open scientific information exchange in advancing molecular evolutionary research.

Reference

1- Ahmad, I., Arif, M., Xu, M., Zhang J., Ding, Y., & Lyu, F. (2023). Therapeutic values and nutraceutical properties of shiitake mushroom (*Lentinula edodes*): A review. Trends in Food Science & Technology. 134,123–135.
2- Kaur, J., Farooqi, H., Chandra, K., & Panda, B.P. (2024). Predicting the bioactive compounds of *Lentinula edodes* and elucidating their interaction with genes associated to obesity through network pharmacology and in-vitro cell-based assay. Heliyon. 10, e27363.
3- Menolli, N. Jr., Sánchez-Ramírez, S., Sánchez-García, M., *et al.* (2022). Global phylogeny of the shiitake mushroom and

related *Lentinula* species uncovers novel diversity and suggests an origin in the Neotropics. Molecular Phylogenetics and Evolution. 173, 107494.

4- Zhang, J., Shen, N., Li, C., *et al*. (2022). Population genomics provides insights into the genetic basis of adaptive evolution in the mushroom-forming fungus *Lentinula edodes*. Journal of Advanced Research. 38, 91–106.

5- Díez, J., Manjón, J.L., & Martin, F. (2002). Molecular phylogeny of the mycorrhizal desert truffles (*Terfezia* and *Tirmania*), host specificity and edaphic tolerance. Mycologia. 94, 247–259.

6- Schoch, C.L., Seifert, K.A., Huhndorf, S., *et al*. (2012). Nuclear ribosomal internal transcribed spacer (ITS) region as a universal DNA barcode marker for fungi. Proceedings of the National Academy of Sciences USA. 109, 6241–6246.

7- Tekpinar, A.D., & Kalmer, A. (2019). Utility of various molecular markers in fungal identification and phylogeny. Nova Hedwigia. 109, 187–224.

8- Cho, M., Heo, Y.M., Jang, Y., Kim, C., Kwon, S.L., & Kim, J.J. (2024). Novel *Sarcoscypha* species from National Parks in Korea: *Sarcoscypha humida* sp. nov. Mycobiology. 52, 51–57.

9- Hawash, M.M., & Al-Shamma, L.M.J. (2025). Analysis of sequences and molecular evolution in the Iraqi date palm cultivars (*Phoenix dactylifera* L.) propagated by tissue culture, based on ITS1 region. Iraqi Journal of Science. 66, 1824–1840.

10- Hawash, M.M., Al-Shahwany, A.W., & Hajeej, T.H.A. (2026). Genetic and Molecular Evolutionary Analysis of Iraqi Figs Using ITS Sequences Compared to some International Cultivars. Iraqi Journal of Science 67(8): 4283-4296

11- Al-Shahwany, A.W., Hawash, M.M., & Hajeej, T.H.A. (2026). Sequence diversity and molecular evolution analysis of international tomato based on the entire ITS region. The Iraqi Journal of Agricultural Sciences. 57, 676–688.

12- Hajeej, T.H.A. (2026). Sequence analysis and molecular evolutionary assessment of *Eucalyptus* spp. across different environmental regions within Baghdad city based on the complete ITS region of nuclear ribosomal DNA. Euphrates Journal of Agricultural Science. 18, 1882–1902.

13- Kwan, H.S., Pang, K.M., Chiu, S.W., & Cheng, S.C. (1992). Nucleotide sequence of the 5.8S ribosomal RNA gene of *Lentinula edodes*. Nucleic Acids Research. 20:610.

14- Edgar, R.C. (2004). MUSCLE: multiple sequence alignment with high accuracy and high throughput. Nucleic Acids Research. 32, 1792–1797.

15- Kumar, S., Stecher, G., Suleski, M., *et al.* (2024). MEGA12: molecular evolutionary genetics analysis version 12 for adaptive and green computing. Molecular Biology and Evolution. 41, msae263.

16- Lorenz, R., Bernhart, S.H., Höner, zu., Siederdissen, C., *et al.* (2011). ViennaRNA Package 2.0. Algorithms for Molecular Biology. 6:26.

17- Bernhart, S.H., Hofacker, I.L., Will, S., Gruber, A.R., & Stadler, P.F. (2008). RNAalifold: improved consensus structure prediction for RNA alignments. BMC Bioinformatics. 2008;9:474.

18- Librado, P., & Rozas, J. (2009). DnaSP v5: a software for comprehensive analysis of DNA polymorphism data. Bioinformatics. 25:1451–1452.

19- French, N., Yu, S., Biggs, P., *et al*. (2014). Evolution of Campylobacter species in New Zealand. In: Sheppard, S.K., Méric, G., editors. Campylobacter Ecology and Evolution. Norfolk: Caister Academic Press; p. 221–240.

20- Leigh, J.W., & Bryant, D. (2015). POPART: full-feature software for haplotype network construction. Methods in Ecology and Evolution. 6, 1110–1116.

21- Barroso, G., Sirand-Pugnet, B., Mouhamadou, B., & Labarère, J. (2003). Secondary structure and molecular evolution of the mitochondrial small subunit ribosomal RNA in Agaricales. Journal of Molecular Evolution. 57, 383–396.

22- Rosenblad, M.A., Martín, M.P., Tedersoo, L., *et al*. (2016). Detection of signal recognition particle (SRP) RNAs in the nuclear ribosomal internal transcribed spacer 1 (ITS1) of three lineages of ectomycorrhizal fungi. MycoKeys. 13, 21–33.

23- Coleman, A.W. (2007). Pan-eukaryote ITS2 homologies revealed by RNA

secondary structure. Nucleic Acids Research. 35, 3322–3329.

24- Sierra-Patev, S., Min, B., Naranjo-Ortiz, M., *et al*. (2023). A global phylogenomic analysis of the shiitake genus *Lentinula*. Proceedings of the National Academy of Sciences USA. 120:e2214076120.

25- Rampersad, S.N. (2014). ITS1, 5.8S and ITS2 secondary structure modelling for intra-specific differentiation among species of the *Colletotrichum gloeosporioides* sensu lato species complex. SpringerPlus. 3:684.

26- Lal, A., Shamim, A., Kil, E.J., *et al*. (2023). Insights into the differential composition of stem-loop structures of nanoviruses and their impacts. Microbiology Spectrum. 11:e04798-22.

27- González, P., & Labarère, J. (2000). Phylogenetic relationships of *Pleurotus* species according to the sequence and secondary structure of the mitochondrial small-subunit rRNA V4, V6 and V9 domains. Microbiology. 146:209–221.

28- Gillespie, J.J. (2004). Characterizing regions of ambiguous alignment caused by the expansion and contraction of hairpin-stem loops in ribosomal RNA molecules. Molecular Phylogenetics and Evolution. 33:936–943.